Characterisation of molecular and cellular CDK9 functions using a novel specific inhibitor

Running title: Novel CDK9 inhibitor

T K Albert[1], C Rigault[1,2], J Eickhoff[3], K Baumgart[1], C Antrecht[1], B Klebl[3], G Mittler[4] and M Meisterernst[1,5]

[1]Institute of Molecular Tumor Biology (IMTB), Faculty of Medicine, Westfalian Wilhelms University Muenster (WWU), 48149 Muenster, Germany

[2]Present Address: Centre des Sciences du Goût et de l'Alimentation, CNRS 6265-INRA 1324-Université de Bourgogne, 21000 Dijon, France

[3]LDC - Lead Discovery Center GmbH, 44227 Dortmund, Germany

[4]Max Planck Institute of Immunobiology and Epigenetics, 79108 Freiburg, Germany

[5]To whom correspondence should be addressed: Michael Meisterernst, Institute of Molecular Tumor Biology, Faculty of Medicine, Westfalian Wilhelms University Muenster, Robert-Koch-Strasse 43, 48149 Muenster, Germany, Email: meistere@uni-muenster.de

This article has been accepted for publication and undergone full peer review but has not been through the copyediting, typesetting, pagination and proofreading process, which may lead to differences between this version and the Version of Record. Please cite this article as doi: 10.1111/bph.12408

Summary

Background and purpose

CDK9 has great potential as therapeutic target. Yet, currently available inhibitors suffer from low specificity and/or narrow therapeutic windows. We present a novel high-specificity CDK9 inhibitor termed 067 that serves to interrogate gene control mechanisms by CDK9 and represents a promising lead for the development of clinically useful mono-specific CDK9 inhibitors.

Experimental approach

CDK9 selectivity of 067 was established in functional kinase assays. CDK9 functions in gene expression were reinvestigated in *in vitro* transcription experiments, single gene analyses and genome-wide expression profiling. Cell-based assays were used to investigate cellular responses to the novel inhibitor.

Key results

The selectivity of 067 for CDK9 exceeded that of the established compounds flavopiridol and DRB by far. 067 inhibited *in vitro* transcription in an ATP-competitive and dose-dependent manner. Gene expression profiling of 067-treated cells revealed selective reduction of short-lived mRNAs, including prominent regulators of proliferation and apoptosis. Analysis of *de novo* RNA synthesis reasoned for a broad positive role of CDK9. At the molecular and cellular level 067 recapitulated known hallmarks of CDK9 inhibition, i.e. enhanced pausing of RNA polymerase II on genes and, most importantly, induction of apoptosis in cancer cells.

Conclusions and implications

Our study provides a framework for the mechanistic understanding of cellular responses to CDK9 inhibition. The data are predictably relevant for biomedical applications.

Keywords

Cyclin-dependent kinase, CDK9, gene expression, RNA polymerase II, transcription

Abbreviations

067: LDC000067

AML: acute myelogenous leukaemia

CDK: cyclin-dependent kinase

ChIP: chromatin immunoprecipitation

CLL: chronic lymphocytic leukaemia

CTD: carboxyterminal domain

DRB: 5,6-dichloro-1-beta-D-ribofuranosyl-benzimidazole

DSIF: DRB sensitivity-inducing factor

FRET: fluorescence resonance energy transfer

hnRNA: heterogeneous nuclear RNA

HPLC-MS: high performance liquid chromatography-mass spectometry

IC_{50}: half-maximal inhibitory concentration

NELF: negative elongation factor

PIC: preinitiation complex

P-TEFb: positive transcription elongation factor b

RMA: robust multi-array average

RNAPII: RNA polymerase II

RT-qPCR: reverse transcription-quantitative real-time PCR

Ser2/5/7-P: CTD phospho-serine 2/5/7

Introduction

Cyclin-dependent kinases (CDKs) are a family of evolutionary conserved serine/threonine kinases that form heterodimers with regulatory cyclin partner proteins (Malumbres and Barbacid, 2005). CDKs can generally be classified into two major groups based on whether they control cell cycle progression or regulate gene transcription by RNA polymerase II (RNAPII). The first group includes CDK1 to CDK6, while CDK8, CDK9, CDK12 and CDK19 are linked to transcription regulation (Loyer *et al.*, 2005). CDK7 and CDK20 act in both cell cycle control and transcription (Fisher, 2005, Wohlbold et al., 2006). Several CDKs (such as CDK10, CDK11A, CDK11B, CDK13) are involved in RNA processing (Loyer *et al.*, 2005), while other CDKs have specialized roles in proliferation and other processes such as cellular survival, homeostasis or development (Malumbres and Barbacid, 2005). Taken together, CDKs present particularly promising drug targets for therapeutic interference in human pathologies where these processes are affected (Malumbres and Barbacid, 2009, Shapiro, 2006), and several CDK inhibitors are currently under evaluation in clinical trials (http://clinicaltrials.gov/). In particular, inhibition of transcriptional CDKs such as CDK9 might present an effective strategy against proliferative diseases like cancer (Shapiro, 2006, Wang and Fischer, 2008). This idea is supported by the observation that cancer cells often rely on the production of short-lived antiapoptotic regulator proteins in order to resist programmed cell death. Transcriptional down-regulation of such survival factors through pharmacological CDK9 inhibition would result in antitumor activity due to reinstatement of apoptosis. Indeed, down-regulation of the antiapoptotic *MCL1* gene by the established CDK9 inhibitor flavopiridol (alvocidib) appears to be the primary mechanism underlying its antitumor activity in chronic lymphocytic leukaemia (CLL) (Byrd et al., 2007, Chen et al., 2005). While these results speak to the potential of CDK9 as a therapeutic target, flavopiridol

has been shown to inhibit multiple CDKs (Liu *et al.*, 2012) as well as other kinases such as AKT (Caracciolo *et al.*, 2012). Thus, inhibitors that exhibit higher specificity for CDK9 are needed to establish final target validation and/or to investigate the underlying molecular mechanisms of gene expression control by CDK9 in greater detail.

CDK9 and cyclin T form the P-TEFb complex that was originally identified as activity controlling the early phase of transcription elongation via release of RNAPII from inherent promoter-proximal pause sites (Li and Gilmour, 2011, Marshall and Price, 1995). This release involves phosphorylation of the inhibitor DSIF, which consists of SPT4 and SPT5 subunits, as well as subunits of negative elongation factor NELF (Fujinaga et al., 2004, Isel and Karn, 1999, Ivanov et al., 2000, Wada et al., 1998, Yamaguchi et al., 1999). DSIF and NELF are thought to cooperate to cause promoter-proximal pausing of RNAPII (Peterlin and Price, 2006, Garriga and Grana, 2004). Subsequent phosphorylation of SPT5 and NELF subunits leads to dissociation of NELF and conversion of DSIF into a positive processivity factor (Martinez-Rucobo et al., 2011, Martinez-Rucobo and Cramer, 2013). CDK9 also phosphorylates the carboxyterminal heptarepeat (consensus sequence $Y_1S_2P_3T_4S_5P_6S_7$) within the carboxyterminal domain (CTD) of the largest subunit of RNAPII. The CTD is modified at various stages of transcription. RNAPII is recruited into the preinitiation complex (PIC) with a hypophosphorylated CTD, and the CTD is phosphorylated on serine 5 (Ser5-P) during initiation and then on serine 2 (Ser2-P) during elongation (Fuda *et al.*, 2009). The latter task is performed by CDK9 (Shim *et al.*, 2002). The degree of phosphorylation at serine 2 increases towards the 3'-ends of genes, which correlates to binding of termination and RNA processing factors to the CTD (Bird *et al.*, 2004). Ser2-P at promoter-proximal sites further helps to release RNAPII from initiation and early elongation complexes (Zhou *et al.*, 2012).

Proteomic studies identified two differently sized forms of P-TEFb, the larger one representing an inactive form of P-TEFb in complex with HEXIM proteins and 7SK RNA

(Nguyen et al., 2001, Yang et al., 2001). Targeting CDK9 with pharmacological inhibitors causes its release from this pool, allowing it to bind to genes either on its own or in combination with other proteins. Investigations of individual cellular and viral genes indicate a widespread positive role for CDK9 in gene control (Chao and Price, 2001, Kanazawa et al., 2000, Lis et al., 2000, Zhu et al., 1997). The requirement for CDK9 may quantitatively differ from one gene to another and/or from one activator to another (Bottardi et al., 2011, Hou et al., 2007, Wang et al., 2013).

Here we introduce a novel inhibitor based on a 2,4-aminopyrimidine scaffold, termed LDC000067 (067), that originates from a small molecule screen of a chemical library that was designed to bind to kinase ATP binding pockets. Functional kinase assays confirmed its selectivity for CDKs, with a preference for CDK9-cyclin T1. 067 inhibited CDK9 *in vitro* with an IC_{50} of 44 ± 10 nM. Its selectivity for CDK9 versus other CDKs was in the range of 55-fold (versus CDK2) to over 230-fold (versus CDK6 and CDK7) and exceeded that of the widely used compounds 5,6-dichloro-1-beta-D-ribofuranosyl-benzimidazole (DRB) and flavopiridol by far. This superior selectivity of 067 was confirmed in an ATP-competitive kinase binding assay. 067 also inhibited *in vitro* transcription in an ATP-competitive and dose-dependent manner. Furthermore, 067 decreased phosphorylation of residue serine 2 within the CTD of RNAPII, both in cells and nuclear extracts as well as in kinase assays using recombinant GST-CTD as substrate. Cellular effects of 067 included induction of the tumor suppressor protein p53 and apoptosis. Gene expression profiling of 067-treated cells revealed selective reduction of short-lived mRNAs, including those that encode regulators of proliferation and apoptosis such as MCL1 and MYC. Analysis of *de novo* RNA synthesis reasoned for a broad positive role of CDK9. Finally, upon 067 treatment the previously proposed forcing of pausing of RNAPII on *MYC* and other genes was observed, all of which is consistent with specific inhibition of CDK9 by 067. In view of these specific properties,

067 may be a valuable tool to further study CDK9 mechanisms of action *in vitro* and *in vivo* as well as a potential drug to target CDK9 in diseases.

Methods

Synthesis of LDC000067 (3-((6-(2-methoxyphenyl)pyrimidin-4-yl)amino)phenyl) methanesulfonamide

Step 1: To a solution of 4,6-dichloropyrimidine (3.38 g; 22.7 mmol) in a mixture of dimethoxyethane (30 mL) and water (6 ml) were successively added 2-methoxyphenylboronic acid (3.45 g; 22.7 mmol), $PdCl_2(PPh_3)_2$ (175 mg; 0.25 mmol), and potassium carbonate (1.69 g; 12.2 mmol). The mixture was stirred for 3 hours at 80°C and at room temperature over night. It was concentrated under reduced pressure. The residue was dissolved in dichloromethane (100 mL), the solution washed with water, dried over $MgSO_4$, and concentrated *in vacuo*. The intermediate 4-chloro-6-(2-methoxyphenyl)pyrimidine was obtained as a pale yellow solid after chromatographic flash purification (silica gel; dichloromethane/methanol gradient 100:0 to 90:10). Yield: 1.97 g (39 %).

Step 2: To a solution of the intermediate from Step 1 (100 mg; 0.453 mmol) in DMF (1 mL) was added (3-aminophenyl) methanesulfonamide (84.3 mg; 0.453 mmol). The mixture was heated for 1 hour at 80°C. It was diluted with water and the solvent removed by lyophilization. The remaining yellow solid was passed through an SCX ion exchange cartridge (eluent 7N ammonia in methanol). After another lyophilization step the pure title compound was obtained as a white powder. Yield: 119.8 mg (71%). ^{1}H NMR (400MHz, d_6-DMSO, 300K) δ 3.88 (s, 3H), 4.24 (s, 2H), 6.84 (bs, 2H), 7.00-7.09 (m, 2H), 7.17 (d, J = 8.4 Hz, 1H), 7.33 (t, J = 7.9 Hz, 1H), 7.42-7.47 (m, 2H), 7.62 (bs, 1H), 7.78-7.82 (m, 1H), 7.91 (dd, J = 1.7 Hz, J = 7.7 Hz, 1H), 8.68 (s, 1H), 9.76 (bs, 1H). MS (ES) $C_{18}H_{18}N_4O_3S$ requires: 370, found: 371 $(M+H)^+$. Purity of the compound was >95% as determined by HPLC-MS.

In vitro enzymatic kinase assay for CDKs

The fluorescence resonance energy transfer (FRET)-based LANCE Ultra KinaSelect Ser/Thr kit (Perkin Elmer) was used to determine IC_{50} values for various CDK inhibitors. Kinase activity and inhibition in this assay was measured as recommended by the manufacturer. Briefly, a specific ULight MBP peptide substrate (50 nM final concentration) was phosphorylated by a CDK-cyclin pair in buffer (50 mM HEPES-KOH pH 7.5, 10 mM $MgCl_2$, 1 mM EGTA, 2 mM dithiothreitol) containing ATP at the concentration of the K_M values of the individual kinases for 1 hour at room temperature. Subsequently, phosphorylation was detected by addition of specific Europium (Eu)-labelled anti-phospho-antibodies (2 nM), which upon binding to the phosphopeptide give rise to a FRET signal. FRET signals were recorded in a time-resolved manner in a Perkin Elmer EnVision reader. Purified cyclin-kinase pairs were obtained from the following suppliers: Carna Biosciences (CDK1-Cyclin B1, CDK6-Cyclin D3, CDK7-Cyclin H-MAT1), ProQinase (CDK2-Cyclin A) and Invitrogen (CDK9-Cyclin T1).

Competitive kinase binding/tracer displacement assay

The LanthaScreen Eu Kinase Binding Assay (Invitrogen) was performed for CDK-cyclin pairs (suppliers: see above) to determine affinities of inhibitors binding to the ATP binding pocket (K_d determination). It is a FRET assay based on binding and displacement of an ATP-competitive tracer to the kinase of interest. Binding of an inhibitor to the kinase competes for binding with the tracer, resulting in a loss of FRET. The assays were performed under the conditions recommended by the supplier. Briefly, inhibitors were incubated for 1 hour with kinase tracer 236 at the concentration corresponding to its individual K_d value for the kinase-cyclin complex, 2 nM LanthaScreen Eu-Anti-His antibody and 5 nM of the purified kinase-cyclin complex. Binding of the tracer to the kinase was measured at 340 nM excitation; 665 nm emission was used for the kinase tracer and 615 nM emission for normalisation.

Kinase panel profiling

Kinase inhibition by 067 was measured in a radiometric assay by Reaction Biology (Malvern, PA, USA). The assay directly measures kinase catalytic activity toward a specific substrate (Anastassiadis *et al.*, 2011). Briefly, 10 µM 067 or DMSO as solvent control were added to Base Reaction Buffer (20 mM Hepes pH 7.5, 10 mM $MgCl_2$, 1 mM EDTA, 0.02% Brij35, 0.02 mg/ml BSA, 0.1 mM Na_3VO_4, 2 mM DTT, 1% DMSO) containing substrates and cofactors required by the individual kinase. ^{33}P-ATP (specific activity 10 µCi/µl) was added to the reaction mixture, and kinase reactions incubated for 120 min at room temperature. Reactions were spotted on P81 ion exchange paper (Whatman), and filters extensively washed in 0.75% phosphoric acid before radiometric quantification. Each protein kinase was measured in duplicate and its catalytic activity expressed as residual kinase activity, i.e. the percentage of average substrate phosphorylation compared to the solvent control reaction.

In vitro transcription

Transcription reactions were conducted with the adenovirus core promoter (template Gal-ML) essentially as described previously (Boeing *et al.*, 2010). For the kinetic elongation assay a slightly modified immobilised Gal-ML template was used, which will be described elsewhere. For immobilisation, templates were PCR amplified using a 5'-biotin-labelled primer that was purified and coupled to paramagnetic streptavidin beads (Promega). Reactions were conducted in 25 mM HEPES-KOH pH 8.2, 60 mM KCl, 5 mM $MgCl_2$, 1 mM DTT, 0.01% Igepal CA-630, 5-10% glycerol, 0.5 mg/ml BSA (Roche Applied Science) and 20 units of RiboLock (Fermentas). Following transcription reactions, beads were washed, RNA eluted, precipitated and analysed on denaturing gels.

DNA microarray analysis

Gene expression profiling was conducted using high-density oligonucleotide arrays (Human Gene 1.0 ST array, Affymetrix). Total RNA was isolated from three biological replicates of 067-treated (90 min) THP1 cells using the RNeasy RNA purification kit as recommended by the supplier (Qiagen). Sample labeling, hybridisation, scanning, raw data extraction and robust multi-array average (RMA) analysis of background-adjusted, normalized, and log-transformed probe-set values were conducted by an authorised Affymetrix service provider (KFB, Regensburg, Germany). Threshold settings for regulated genes were ≥1.4-fold difference to DMSO-treated control cells, with $p < 0.05$. Gene ontology analysis of regulated genes was performed with DAVID (http://david.abcc.ncifcrf.gov/).

Reverse transcription quantitative PCR (RT-qPCR)

Total RNA was prepared using Trizol reagent (Invitrogen). Reverse transcription was performed using either Superscript II reverse transcriptase (Invitrogen) or Quantitect reverse transcription kit (Qiagen) with random hexamer primers. Quantitative real-time PCR (qPCR) was carried out on the resulting cDNAs using SYBR Green PCR Master kit (Applied Biosystems) according to manufacturers instructions on a Step One Plus PCR system (Applied Biosystems). Relative transcripts levels were determined using the comparative cycle threshold ($\Delta\Delta C_T$) method. Exon-intron primers were designed with the program Primer3 (http://primer3.wi.mit.edu/). Sequences are available upon request.

Chromatin immunoprecipitation (ChIP) and antibodies

ChIP was performed as previously described (Albert *et al.*, 2010). ChIP and input DNAs were purified with the Qiaquick PCR kit (Qiagen), and qPCR was carried out as outlined above. Antibodies used included IgG control (sc-2027), anti-RNAPII, subunit RPB1 (sc-899), anti-

CDK9 (sc-484; all from Santa Cruz Biotechnology), and monoclonal rat antibodies anti-CTD Ser2-P (clone 3E10), anti-Ser5-P (3E8), and anti-Ser7-P (4E12; all kind gifts from D. Eick). Additional antibodies for Western blot analyses included anti-p53 phospho-serine 392 (sc-56173) and anti-Tubulin (sc-8035; Santa Cruz Biotechnology).

Apoptosis measurement

Apoptosis was measured by flow cytometry using annexin-fluorescein and propidium iodide staining according to standard protocols (BD Biosciences).

Results

LDC000067, a novel CDK inhibitor with high specificity for CDK9

Given the limited specificity of several widely used CDK9 inhibitors we set out to develop highly specific ATP-competitive compounds based on a 2,4-aminopyrimidine scaffold. Specificity was increased in iterative cycles of chemical modification and validated by functional kinase assays. As an intermediate endpoint we present here the CDK9 inhibitor 067 (patent number WO 2008/129080; Fig. 1A), which shows promising biochemical and pharmacological properties including high selectivity for CDK9, high stability as well as good tolerability and low cytotoxicity *in vivo*.

The increased CDK9 selectivity of 067 in comparison to established CDK inhibitors flavopiridol, DRB and SNS-032 (formerly BMS-387032) (Misra *et al.*, 2004) was demonstrated via substrate phosphorylation using a fluorescence resonance energy transfer (FRET)-based assay. Half-maximal inhibitory concentrations (IC_{50}) for the CDK9-cyclin T1 pair were 44 nM, 5.2 nM, 1.4 nM and 1.9 µM for 067, flavopiridol, SNS-032 and DRB,

respectively (Table 1). Importantly, in this assay 067 displayed 55/125/210/>227/>227-fold selectivity for CDK9 versus CDK2/1/4/6/7, while the other three compounds were much less selective (e.g. 3/<1/7/59/20-fold for CDK9 versus CDK2/1/4/6/7 in the case of flavopiridol). High CDK9 selectivity of 067 was confirmed via another FRET-based *in vitro* assay where the ATP-competitive binding of 067, flavopiridol and DRB to CDK2-, CDK7- and CDK9-cyclin complexes was compared (Table 2). The dissociation constant of 067 for CDK9-cyclin T1 was 31-fold lower than for CDK2-cyclin A and nearly 500-fold lower than for the trimeric CDK7-cyclin H-MAT1 complex; again, flavopiridol and DRB showed lower relative differences in their dissociation constants for these CDKs. Since the IC_{50} of 067 for CDK2 is 55-fold and its K_d 31-fold higher than the corresponding values for CDK9, it seems unlikely that 067 has a significant effect on CDK2 function when employed at the concentrations required to block CDK9 function.

Further support for the selectivity of 067 was obtained by profiling a panel of 28 additional human recombinant non-CDK kinases for their response to 067. In this radiometric assay, 10 µM 067 or DMSO as solvent control were added to a kinase reaction that directly measures catalytic activity of the enzyme toward a specific substrate (Anastassiadis *et al.*, 2011). 22 out of the 28 kinases showed greater than 50% residual activity in the presence of 067, while CDK9-Cyclin T1 was severely affected (6% residual activity; Figure 1 B). In an additional experiment, comparative IC_{50} values for several of the less affected kinases (e.g. GSK3A, MAP4K4 or ABL2 with 9.5%, 17.5% and 27% residual activity, respectively) were determined for 067 versus staurosporine, a prototypical ATP-competitive kinase inhibitor that is known to bind to many kinases with high affinity but little selectivity (Karaman *et al.*, 2008). Strikingly, IC_{50} values were several hundred fold higher than the ones obtained with the non-selective inhibitor staurosporine (Table 3).

067 inhibits P-TEFb-dependent in vitro transcription in an ATP-competitive manner

We next asked whether 067 blocks transcription in a similar way to DRB and flavopiridol. *In vitro* transcription experiments were conducted using either soluble or immobilised promoter templates (Boeing *et al.*, 2010) and nuclear extracts of HEK293T cells supplemented with recombinant Gal4-VP16. Transcription assays revealed a half-maximal inhibition of 4 μM for 067 at 100 μM ATP (Fig. 1B). Using the same assay a roughly 20-fold higher potency of flavopiridol and a 2.5-fold lower potency of DRB was revealed (Fig. 1C). Nuclear extracts from four different cell lines were used to investigate the influence of ATP concentrations on 067-dependent inhibition of transcription activity (Fig. 1D). For these and most subsequent experiments a final concentration of 10 μM was chosen which reduces transcription levels to approximately 20-30% *in vitro* as well as *in vivo* (see below). High ATP levels (500 μM) markedly diminished the inhibitory effect of 067 on *in vitro* transcription when compared to the routinely used 60 μM ATP. ATP competition was not unexpected, since (i) 067 emerged from a chemical library containing scaffolds designed for binding to kinase ATP binding sites, and (ii) 067 competed with/displaced the tracer from the ATP binding pocket in the *in vitro* kinase binding assay (Table 2). We further investigated the effects of potassium or magnesium chloride on the relative inhibitory potency of 067. While increasing the concentration of KCl from the routinely used 50 mM up to 150 mM resulted in a strong overall decrease of transcript levels, the relative inhibitory potency of 067 was largely unaffected (KB, data not shown). In contrast, adding increasing amounts of $MgCl_2$ during the transcription elongation resulted in a significant Mg^{2+}-dependent decrease of transcriptional inhibition by 067 (Fig. 1E).

CDK9 inhibition by 067 reduces Ser2-P, induces p53 activation and leads to apoptosis

Next the effects of CDK9 inhibition by 067 in living cells were investigated. One established cellular target of CDK9 is serine 2 within the RNA polymerase CTD which becomes phosphorylated during transcription elongation (Fuda *et al.*, 2009). Previous experiments in mouse embryonic stem cells (mESCs) had shown that flavopiridol at 1 µM significantly reduced Ser2-P levels within 90 minutes (Rahl *et al.*, 2010). We therefore compared the effects of 067 versus flavopiridol treatment in mESCs. Cells were treated with either 10 µM 067 or 1 µM flavopiridol for 90 and 180 minutes and subsequently analysed by Western blot. Treatment with the two compounds led to 1.6-fold and 3.4-fold reduction of Ser2-P after 90 minutes (Fig. 2A). While Ser2-P repression remained at the same level for 067 after 180 minutes, flavopiridol treatment nearly abolished the CTD modification at the later time point. This quantitative difference might be attributed to the very high concentration of flavopiridol which could result in non-specific effects especially at later time points (see discussion). We also compared the effects of 067 treatment on CTD phosphorylation to the other widely used CDK9 inhibitor DRB in HeLa cells (Fig. 2B). Again, a 60 min treatment with 10 µM 067 resulted in 1.6-fold reduction of Ser2-P, whereas Ser5-P and Ser7-P remained largely unaffected; this reduction was similar to the one obtained with 50 µM DRB. Finally, we confirmed these results in an *in vitro* kinase assay using recombinant GST-CTD as substrate in HeLa nuclear extracts (Fig. 2C).

Blocking RNAPII transcription elicits a stress response that leads to activation of p53 (Ljungman *et al.*, 1999). During this process p53 is stabilised and becomes activated by a plethora of post-translational modifications, e.g. extensive phosphorylation. Next we examined the effect of 067 on p53 signaling. Given that p53 is frequently mutated or inactive in tumour cells (one example is HeLa) we used the breast carcinoma cell line MCF7, in which p53 signaling is preserved. Indeed, after four hours treatment with 10 µM 067 (or 50 µM DRB), the p53 protein was stabilised (data not shown) and activated as monitored by

phosphorylation of serine 392 (Fig. 2D), a modification that is an integral event in the induction of p53 by a diverse range of stimuli (Cox and Meek, 2010).

Various cell lines, in particular of haematopoietic origin, show pronounced sensitivity to flavopiridol- and/or DRB-induced apoptosis (Konig et al., 1997, Parker et al., 1998, te Poele et al., 1999). Due to its proapoptotic effects flavopiridol is currently under investigation in phase II clinical trials as therapeutic agent in acute myelogenous leukaemia (AML) (Karp *et al*., 2012). We tested the effects of 067 treatment on several cancer cell lines as well as on primary patient-derived AML blasts using flow cytometry of annexin V-propidium iodide double-stained cells (Fig. 2E-H). At concentrations >2 μM all cells showed a marked increase in the percentage of apoptotic cells after 24 hours of exposure (Fig. 2E). Apoptosis induction was most pronounced in cells of leukaemic origin such as THP1 (approximately 45% apoptotic cells at 10 μM 067) and patient-derived blast cells (>60% at 10 μM). Titration of 067 in epithelial A549 lung carcinoma cells revealed near-saturation concentrations above 15 μM, with a 3-fold increase in apoptosis observed at 10 μM (Fig. 2F). 067 treatment of HCT116 colon carcinoma cells which either contained or lacked wild-type p53 caused a similar degree of apoptosis induction in both situations, suggesting a largely p53-independent mechanism at least in this cellular background (Fig. 2G). Finally, comparison of cell death rates in 067-treated (10 μM) or flavopiridol-treated (0.25 μM) A549 and MCF7 cells revealed a similar degree of apoptosis induction (Fig. 2H). Taken together, these data indicate that 067 treatment of cells recapitulates several relevant cellular responses to CDK9 inhibition, most importantly induction of programmed cell death in leukaemia cells.

Dose-dependent inhibition of de novo RNA synthesis by 067

To quantitatively determine the effects of 067 on gene transcription *in vivo*, a concentration-dependent analysis of mRNA synthesis was conducted. Cells were treated with the inhibitor

for 90 minutes, RNA was extracted and mRNA analysed via reverse transcription-quantitative real-time PCR (RT-qPCR) at several representative cellular genes, including housekeeping genes such as *GAPDH* and *RPL3*, cell cycle control genes such as *p21*, cyclin D1/*CCND1*, *PLK2*, or the *MYC* gene (Fig. 3A). As newly synthesised RNA is rapidly spliced (within minutes), and mature mRNA can be stable over days, we chose to analyse *de novo* synthesised hnRNA using primer pairs located in neighbouring exon and intron regions. Repression of mRNA synthesis was first detectable at a concentration of 1 μM, with 50% to 80% repression obtained at a concentration of 10 μM 067. Half-maximal repression by 067 was achieved in the range of 2 to 6 μM. While relative changes were comparable, the final level of repression varied from gene to gene (Fig. 3A). Notably, housekeeping genes (*GAPDH*, *RPL3*) were among the strongest responders. Similar results were obtained in several human cancer cell lines (e.g. HeLa, THP1; data not shown) as well as in mESCs (Fig. 3B). Occasionally we observed moderate stimulatory effects, for instance on *Myc* in mESCs, yet these were restricted to low concentrations of 067. The underlying reason remains unclear.

De novo RNA synthesis was also measured using a Tetracyclin-inducible luciferase reporter gene system in HeLa cells (Boeing et al., 2010, Uhlmann et al., 2007). Treatment with 10 μM 067 caused an 80% to 90% reduction of RNA synthesis (Fig. 3C). Luciferase expression decreased in a concentration-dependent manner, with half-maximal repression reached at a 067 concentration of 2 μM (Fig. 3D). Luciferase repression was stable over at least three days, indicating that 067 was not metabolised to an inactive form but remained fully active inside the cells (Fig. 3D). Together, these data classify 067 as an inhibitor of *de novo* RNA synthesis by RNA polymerase II that is effective at low micromolar concentrations.

P-TEFb broadly affects RNA synthesis of cellular genes

Microarray gene expression profiling was conducted on RNA isolated from cells treated for 90 min with 067 (Suppl. Data Set 1). For this analysis we used the leukaemia cell line THP1 transformed by MLL-AF9, as it had shown high sensitivity for CDK9 inhibition by 067 (c.f. Fig. 2E). Approximately 1,300 or 4.5% of all genes were reproducibly regulated by 067 (three biological replicates; fold ≥1.4; p ≤0.05), out of which 94% were downregulated (Fig. 4A). Within the top responders of the latter group were immediate early genes *MYC* (7-fold down-regulated) and *FOS* (5-fold down). Other genes found were M-phase regulatory kinases *PLK2/3/4*, chromosome segregation proteins *CENPL/C1*, anti-proliferative genes *BTG1/2* and, consistent with the observed induction of apoptosis, *MCL1*, all of which were previously identified as targets of flavopiridol and/or DRB (Lam et al., 2001, Garriga et al., 2010). Interestingly, several miRNA genes, including *miR-15a*, *miR-21*, *let-7f*, the polycistronic *MYC*-controlled *miR-17-92 ONCOMIR* cluster (Esquela-Kerscher and Slack, 2006), and at least 106 non-coding RNA genes were shown to be downregulated. Approximately 80% of the latter group represent small nucleolar RNAs (snoRNAs), many of which are located in the introns of protein-coding genes that are subject to rapid splicing (Filipowicz and Pogacic, 2002). These data are generally consistent with and extend previous data from microarray analyses using well-established CDK9 inhibitors such as flavopiridol or DRB.

Gene ontology analysis indicated an over-representation of transcription factors with fast-decaying mRNAs in the group of downregulated genes (Yang *et al.*, 2003) (Fig. 4B). We hypothesised that genes with intrinsically stable mRNA might remain unaffected in the microarrays. To investigate this possibility, *de novo* RNA synthesis was analysed at nine genes that were shown not to be affected by 067 in the microarrays. This group of genes, which included the housekeeping genes *RPS15*, *RPL31* or *MED1*, showed a significant decrease in their unspliced transcript levels (Fig. 4C). The projection of these and the previous RT-qPCR analyses (Fig. 3) suggests that CDK9 positively controls mRNA synthesis of many

more genes than was initially deducible from gene expression array data, in which RNA stability appears to confer experimental bias.

CDK9 inhibition by 067 increases promoter-proximal RNAPII levels

CDK9 alleviates promoter-proximal pausing of RNAPII (Zhou *et al.*, 2012). Release of the polymerase from these positions is mediated through CTD phosphorylation as well as via release of the inhibitory factors SPT5 and NELF (Yamaguchi *et al.*, 1999). Correspondingly, CDK9 inhibition by DRB or flavopiridol results in elevated RNAPII levels at promoter-proximal pause sites (Glover-Cutter et al., 2008, Rahl et al., 2010). We next addressed whether and how transcriptional inhibition by 067 would correlate to the distribution of RNAPII at the prototypical paused *MYC* gene by conducting chromatin immunoprecipitation (ChIP) analysis in 067-treated HeLa cells (Fig. 5). In line with the previous reports, 067 forced RNAPII to pause in a promoter-proximal position (Fig. 5A). Total RNAPII, and those forms with a phosphorylated CTD at position serine 5 (Fig. 5D) and serine 7 (Fig. 5E) moderately increased at promoter-proximal sites. Conversely, phosphorylation of the CTD at serine 2 was low at the 5'-end of the *MYC* gene and steadily increased towards the 3'-end (Fig. 5C). The influence of 067 on serine 2 phosphorylation was surprisingly moderate under conditions where *MYC* transcription was reduced to less than 50% (compare Fig. 3A). Of further note, RNAPII levels in the 3'-region of the gene remained relatively high in the presence of 067. Similar ChIP analyses of other genes and/or in other cells confirmed the above above findings, i.e. increased RNAPII levels predominantly at the 5'-end of genes (data not shown). Taken together, our data illustrate the situation of CDK9 inhibition by a dynamic, ATP-competitive inhibitor at intermediate non-saturating conditions. It is likely relevant from a mechanistic point of view as well as for potential applications as it illuminates the response of RNAPII under limiting (but not eradicated) CDK9 activity.

Discussion and Conclusions

In the current study we introduce a novel inhibitor and characterise it as a highly selective binder of CDK9 that effectively interferes with the RNA synthesis of many genes. 067 is significantly more specific for CDK9 than both flavopiridol and DRB (Tables 1 and 2), and it has a particular advantage over the latter in that it can be used for biomedical studies in mice (BK, unpublished observations). High CDK9 specificity is especially important in this context since former studies performed with DRB or flavopiridol could have been compromised by the known off-target effects for the other CTD kinases CDK1, CDK2 as well as CDK7.

Using this highly specific inhibitor we have confirmed a series of functions and mechanisms that were previously associated with CDK9, namely (i) the general requirement of CDK9 for efficient transcription *in vitro* (Fig. 1) as well as *in vivo* (Figs. 3 and 4), (ii) the targeting of CTD residue serine 2 by CDK9 (Fig. 2), (iii) the activation of the tumour suppressor p53 (Fig. 2), (iv) the induction of apoptosis (Fig. 2) and (v) the enhancement of RNAPII pausing (Fig. 5) upon selective CDK9 inhibition by 067. *In vivo* RNA analysis carried out in the present study uncovered a critical positive role for CDK9 in the *de novo* RNA synthesis of all analysed genes. Relevant to therapeutic applications, 067 causes apoptosis in several human cancer cell lines (THP1, A549, MCF7, HeLa), as has been previously observed for other CDK9 inhibitors (Fig. 2). In addition, primary AML blasts isolated from leukaemia patients undergo apoptosis upon treatment with 067. Cell death does not depend on active p53 - a similar effect of 067 was observed in HCT116 cells lacking a p53 gene. Instead, we assume that cell death relates to the repression of anti-apoptotic genes such as *MCL1*, which was observed to be downregulated in our microarray studies and has been reported previously in a different context (Lam et al., 2001, Ma et al., 2003). Beyond this, our data generally imply that other genes like *MCL1* that encode mRNAs and proteins

with short half-lives could determine the initial biological response to CDK9 inhibitors. One prominent example is MYC, whose mRNA and protein are subject to rapid turnover (e.g. Fig. 3, and data not shown). Our microarray analysis uncovered additional, novel CDK9 targets, most notably several non-coding RNAs including cancer-associated miRNA genes such as *miR-15a, miR-21, let-7f* (Esquela-Kerscher and Slack, 2006), and the polycystronic *miR-17-92 ONCOMIR* cluster (He *et al.*, 2005). Notably, the latter is a direct target of MYC, suggesting that *ONCOMIR* downregulation (2.2-fold) was mediated through transcriptional repression of *MYC* (O'Donnell *et al.*, 2005).

Our *in vitro* transcription analysis clearly revealed competition between 067 and ATP (Fig. 1D). Surprisingly, CDK9 inhibition by 067 was also strongly dependent on magnesium (Fig. 1E). Currently, we can only speculate about the underlying mechanism. Recent structure-function analyses of the closely related CDK2 demonstrated the requirement for coordination of a second Mg^{2+} ion in the active site to stabilize ATP-binding and to maximally enhance catalytic activity (Bao et al., 2011, Jacobsen et al., 2012). In analogy, CDK9 active site chemistry might depend on this mechanism, too. In this scenario, increasing the availability of magnesium might favour ATP- over 067-binding to the catalytic center of CDK9, thereby diminishing the inhibitory activity of 067.

Reduction of RNAPII CTD phosphorylation at serine 2 by 067 was moderate in comparison with the clinically evaluated flavopiridol, especially after longer drug exposure (Fig. 2A). Of note, reduction in CTD phosphorylation by flavopiridol can not always be directly linked with MCL1 ablation (Shapiro, 2006). On the other hand, abrogation of *MCL1* expression and concurrent apoptosis induction is thought to be the critical mode of action for flavopiridol in chronic lymphocytic leukemia cells (Chen *et al.*, 2005), indicating that Ser2-P is neither the sole (nor likely the most critical) target of CDK9 inhibitors. The more severe effects of flavopiridol on Ser2-P might result from its lower specificity for CDK9. For

example, the pan-specific flavopiridol could target additional CTD-Ser2 kinases such as CDK12 and/or CDK13 (Bartkowiak et al., 2010, Blazek et al., 2011). Alternatively, Ser2-P ablation by flavopiridol could simply reflect its higher affinity toward CDK9 (Table 2) (Chao *et al.*, 2000). Improvement of the comparably low affinity of 067 might help to illuminate this issue in the future.

One important rationale for the development of 067 and related compounds is that pan-CDK inhibitors such as flavopiridol exhibit a significant and dose-limiting level of cytotoxicity (Shapiro, 2006), possibly due to their equipotent inhibition of multiple CDK family members (see e.g. Table 1). This is predictably different for mono- or dual-selective CDK inhibitors. Indeed, using 067 and analogous compounds from the series of aminopyrimidines we could demonstrate that they exhibit a significant therapeutic window (i.e. ratio of toxic-to-efficacious dose) in cells as well as *in vivo* (BK, unpublished observations). Along the same line, a dual-selective CDK4/6 inhibitor (Fry *et al.*, 2004) has recently yielded very encouraging results in a breast cancer trial (Guha, 2013), demonstrating that the selective inhibition of certain CDK family members is a valid therapeutic principle. Taken together, our data provide a rationale for the development and optimization of clinically useful, highly selective CDK9 inhibitors based on the 2,4-aminopyrimidine scaffold, and 067 represents a promising lead in this context.

Acknowledgements

We thank Dirk Eick for CTD antibodies. We are grateful to Tim Kelso for critical reading of the manuscript and other members of the Meisterernst laboratory for helpful discussions. This work was supported by the Ministry for Research and Technology (BMBF, grant number 0313860D to MM and 0313860B to GM) and by grants of the Westfalian Wilhelms University Muenster to MM.

References

ALBERT, T. K., GROTE, K., BOEING, S. & MEISTERERNST, M. (2010) Basal core promoters control the equilibrium between negative cofactor 2 and preinitiation complexes in human cells. *Genome Biol,* 11**,** R33.

ANASTASSIADIS, T., DEACON, S. W., DEVARAJAN, K., MA, H. & PETERSON, J. R. (2011) Comprehensive assay of kinase catalytic activity reveals features of kinase inhibitor selectivity. *Nat Biotechnol,* 29**,** 1039-45.

BAO, Z. Q., JACOBSEN, D. M. & YOUNG, M. A. (2011) Briefly bound to activate: transient binding of a second catalytic magnesium activates the structure and dynamics of CDK2 kinase for catalysis. *Structure,* 19**,** 675-90.

BARTKOWIAK, B., LIU, P., PHATNANI, H. P., FUDA, N. J., COOPER, J. J., PRICE, D. H. *et al.* (2010) CDK12 is a transcription elongation-associated CTD kinase, the metazoan ortholog of yeast Ctk1. *Genes Dev,* 24**,** 2303-16.

BIRD, G., ZORIO, D. A. & BENTLEY, D. L. (2004) RNA polymerase II carboxy-terminal domain phosphorylation is required for cotranscriptional pre-mRNA splicing and 3'-end formation. *Mol Cell Biol,* 24**,** 8963-9.

BLAZEK, D., KOHOUTEK, J., BARTHOLOMEEUSEN, K., JOHANSEN, E., HULINKOVA, P., LUO, Z. *et al.* (2011) The Cyclin K/Cdk12 complex maintains genomic stability via regulation of expression of DNA damage response genes. *Genes Dev,* 25**,** 2158-72.

BOEING, S., RIGAULT, C., HEIDEMANN, M., EICK, D. & MEISTERERNST, M. (2010) RNA polymerase II C-terminal heptarepeat domain Ser-7 phosphorylation is established in a mediator-dependent fashion. *J Biol Chem,* 285**,** 188-96.

BOTTARDI, S., ZMIRI, F. A., BOURGOIN, V., ROSS, J., MAVOUNGOU, L. & MILOT, E. (2011) Ikaros interacts with P-TEFb and cooperates with GATA-1 to enhance transcription elongation. *Nucleic Acids Res,* 39**,** 3505-19.

BYRD, J. C., LIN, T. S., DALTON, J. T., WU, D., PHELPS, M. A., FISCHER, B. *et al.* (2007) Flavopiridol administered using a pharmacologically derived schedule is associated with marked clinical efficacy in refractory, genetically high-risk chronic lymphocytic leukemia. *Blood,* 109**,** 399-404.

CARACCIOLO, V., LAURENTI, G., ROMANO, G., CARNEVALE, V., CIMINI, A. M., CROZIER-FITZGERALD, C. *et al.* (2012) Flavopiridol induces phosphorylation of AKT in a human glioblastoma cell line, in contrast to siRNA-mediated silencing of Cdk9: Implications for drug design and development. *Cell Cycle,* 11**,** 1202-16.

CHAO, S. H., FUJINAGA, K., MARION, J. E., TAUBE, R., SAUSVILLE, E. A., SENDEROWICZ, A. M. *et al.* (2000) Flavopiridol inhibits P-TEFb and blocks HIV-1 replication. *J Biol Chem,* 275**,** 28345-8.

CHAO, S. H. & PRICE, D. H. (2001) Flavopiridol inactivates P-TEFb and blocks most RNA polymerase II transcription in vivo. *J Biol Chem,* 276**,** 31793-9.

CHEN, R., KEATING, M. J., GANDHI, V. & PLUNKETT, W. (2005) Transcription inhibition by flavopiridol: mechanism of chronic lymphocytic leukemia cell death. *Blood,* 106**,** 2513-9.

COX, M. L. & MEEK, D. W. (2010) Phosphorylation of serine 392 in p53 is a common and integral event during p53 induction by diverse stimuli. *Cell Signal,* 22**,** 564-71.

ESQUELA-KERSCHER, A. & SLACK, F. J. (2006) Oncomirs - microRNAs with a role in cancer. *Nat Rev Cancer,* 6**,** 259-69.

FILIPOWICZ, W. & POGACIC, V. (2002) Biogenesis of small nucleolar ribonucleoproteins. *Curr Opin Cell Biol,* 14**,** 319-27.

FISHER, R. P. (2005) Secrets of a double agent: CDK7 in cell-cycle control and transcription. *J Cell Sci,* 118**,** 5171-80.

FRY, D. W., HARVEY, P. J., KELLER, P. R., ELLIOTT, W. L., MEADE, M., TRACHET, E. *et al.* (2004) Specific inhibition of cyclin-dependent kinase 4/6 by PD 0332991 and associated antitumor activity in human tumor xenografts. *Mol Cancer Ther,* 3**,** 1427-38.

FUDA, N. J., ARDEHALI, M. B. & LIS, J. T. (2009) Defining mechanisms that regulate RNA polymerase II transcription in vivo. *Nature,* 461**,** 186-92.

FUJINAGA, K., IRWIN, D., HUANG, Y., TAUBE, R., KUROSU, T. & PETERLIN, B. M. (2004) Dynamics of human immunodeficiency virus transcription: P-TEFb phosphorylates RD and dissociates negative effectors from the transactivation response element. *Mol Cell Biol,* 24**,** 787-95.

GARRIGA, J. & GRANA, X. (2004) Cellular control of gene expression by T-type cyclin/CDK9 complexes. *Gene,* 337**,** 15-23.

GARRIGA, J., XIE, H., OBRADOVIC, Z. & GRANA, X. (2010) Selective control of gene expression by CDK9 in human cells. *J Cell Physiol,* 222**,** 200-8.

GLOVER-CUTTER, K., KIM, S., ESPINOSA, J. & BENTLEY, D. L. (2008) RNA polymerase II pauses and associates with pre-mRNA processing factors at both ends of genes. *Nat Struct Mol Biol,* 15**,** 71-8.

GUHA, M. (2013) Blockbuster dreams for Pfizer's CDK inhibitor. *Nat Biotechnol,* 31**,** 187.

HE, L., THOMSON, J. M., HEMANN, M. T., HERNANDO-MONGE, E., MU, D., GOODSON, S. *et al.* (2005) A microRNA polycistron as a potential human oncogene. *Nature,* 435**,** 828-33.

HOU, T., RAY, S. & BRASIER, A. R. (2007) The functional role of an interleukin 6-inducible CDK9.STAT3 complex in human gamma-fibrinogen gene expression. *J Biol Chem,* 282**,** 37091-102.

ISEL, C. & KARN, J. (1999) Direct evidence that HIV-1 Tat stimulates RNA polymerase II carboxyl-terminal domain hyperphosphorylation during transcriptional elongation. *J Mol Biol,* 290**,** 929-41.

IVANOV, D., KWAK, Y. T., GUO, J. & GAYNOR, R. B. (2000) Domains in the SPT5 protein that modulate its transcriptional regulatory properties. *Mol Cell Biol,* 20**,** 2970-83.

JACOBSEN, D. M., BAO, Z. Q., O'BRIEN, P., BROOKS, C. L., 3RD & YOUNG, M. A. (2012) Price to be paid for two-metal catalysis: magnesium ions that accelerate chemistry unavoidably limit product release from a protein kinase. *J Am Chem Soc,* 134**,** 15357-70.

KANAZAWA, S., OKAMOTO, T. & PETERLIN, B. M. (2000) Tat competes with CIITA for the binding to P-TEFb and blocks the expression of MHC class II genes in HIV infection. *Immunity,* 12**,** 61-70.

KARAMAN, M. W., HERRGARD, S., TREIBER, D. K., GALLANT, P., ATTERIDGE, C. E., CAMPBELL, B. T. *et al.* (2008) A quantitative analysis of kinase inhibitor selectivity. *Nat Biotechnol,* 26**,** 127-32.

KARP, J. E., GARRETT-MAYER, E. L., ESTEY, E. H., RUDEK, M. A., SMITH, B. D., GREER, J. M. *et al.* (2012) Randomized phase II study of two schedules of flavopiridol given as timed sequential therapy with cytosine arabinoside and mitoxantrone for adults with newly diagnosed, poor-risk acute myelogenous leukemia. *Haematologica*.

KONIG, A., SCHWARTZ, G. K., MOHAMMAD, R. M., AL-KATIB, A. & GABRILOVE, J. L. (1997) The novel cyclin-dependent kinase inhibitor flavopiridol downregulates

Bcl-2 and induces growth arrest and apoptosis in chronic B-cell leukemia lines. *Blood,* 90**,** 4307-12.

LAM, L. T., PICKERAL, O. K., PENG, A. C., ROSENWALD, A., HURT, E. M., GILTNANE, J. M. *et al.* (2001) Genomic-scale measurement of mRNA turnover and the mechanisms of action of the anti-cancer drug flavopiridol. *Genome Biol,* 2**,** RESEARCH0041.

LI, J. & GILMOUR, D. S. (2011) Promoter proximal pausing and the control of gene expression. *Curr Opin Genet Dev,* 21**,** 231-5.

LIS, J. T., MASON, P., PENG, J., PRICE, D. H. & WERNER, J. (2000) P-TEFb kinase recruitment and function at heat shock loci. *Genes Dev,* 14**,** 792-803.

LIU, X., SHI, S., LAM, F., PEPPER, C., FISCHER, P. M. & WANG, S. (2012) CDKI-71, a novel CDK9 inhibitor, is preferentially cytotoxic to cancer cells compared to flavopiridol. *Int J Cancer,* 130**,** 1216-26.

LJUNGMAN, M., ZHANG, F., CHEN, F., RAINBOW, A. J. & MCKAY, B. C. (1999) Inhibition of RNA polymerase II as a trigger for the p53 response. *Oncogene,* 18**,** 583-92.

LOYER, P., TREMBLEY, J. H., KATONA, R., KIDD, V. J. & LAHTI, J. M. (2005) Role of CDK/cyclin complexes in transcription and RNA splicing. *Cell Signal,* 17**,** 1033-51.

MA, Y., CRESS, W. D. & HAURA, E. B. (2003) Flavopiridol-induced apoptosis is mediated through up-regulation of E2F1 and repression of Mcl-1. *Mol Cancer Ther,* 2**,** 73-81.

MALUMBRES, M. & BARBACID, M. (2005) Mammalian cyclin-dependent kinases. *Trends Biochem Sci,* 30**,** 630-41.

MALUMBRES, M. & BARBACID, M. (2009) Cell cycle, CDKs and cancer: a changing paradigm. *Nat Rev Cancer,* 9**,** 153-66.

MARSHALL, N. F. & PRICE, D. H. (1995) Purification of P-TEFb, a transcription factor required for the transition into productive elongation. *J Biol Chem,* 270**,** 12335-8.

MARTINEZ-RUCOBO, F. W. & CRAMER, P. (2013) Structural basis of transcription elongation. *Biochim Biophys Acta,* 1829**,** 9-19.

MARTINEZ-RUCOBO, F. W., SAINSBURY, S., CHEUNG, A. C. & CRAMER, P. (2011) Architecture of the RNA polymerase-Spt4/5 complex and basis of universal transcription processivity. *Embo J,* 30**,** 1302-10.

MISRA, R. N., XIAO, H. Y., KIM, K. S., LU, S., HAN, W. C., BARBOSA, S. A. *et al.* (2004) N-(cycloalkylamino)acyl-2-aminothiazole inhibitors of cyclin-dependent kinase 2. N-[5-[[[5-(1,1-dimethylethyl)-2-oxazolyl]methyl]thio]-2-thiazolyl]-4-piperidinecarboxamide (BMS-387032), a highly efficacious and selective antitumor agent. *J Med Chem,* 47**,** 1719-28.

NGUYEN, V. T., KISS, T., MICHELS, A. A. & BENSAUDE, O. (2001) 7SK small nuclear RNA binds to and inhibits the activity of CDK9/cyclin T complexes. *Nature,* 414**,** 322-5.

O'DONNELL, K. A., WENTZEL, E. A., ZELLER, K. I., DANG, C. V. & MENDELL, J. T. (2005) c-Myc-regulated microRNAs modulate E2F1 expression. *Nature,* 435**,** 839-43.

PARKER, B. W., KAUR, G., NIEVES-NEIRA, W., TAIMI, M., KOHLHAGEN, G., SHIMIZU, T. *et al.* (1998) Early induction of apoptosis in hematopoietic cell lines after exposure to flavopiridol. *Blood,* 91**,** 458-65.

PETERLIN, B. M. & PRICE, D. H. (2006) Controlling the elongation phase of transcription with P-TEFb. *Mol Cell,* 23**,** 297-305.

RAHL, P. B., LIN, C. Y., SEILA, A. C., FLYNN, R. A., MCCUINE, S., BURGE, C. B. *et al.* (2010) c-Myc regulates transcriptional pause release. *Cell,* 141**,** 432-45.

SHAPIRO, G. I. (2006) Cyclin-dependent kinase pathways as targets for cancer treatment. *J Clin Oncol,* 24**,** 1770-83.

SHIM, E. Y., WALKER, A. K., SHI, Y. & BLACKWELL, T. K. (2002) CDK-9/cyclin T (P-TEFb) is required in two postinitiation pathways for transcription in the C. elegans embryo. *Genes Dev,* 16**,** 2135-46.

TE POELE, R. H., OKOROKOV, A. L. & JOEL, S. P. (1999) RNA synthesis block by 5, 6-dichloro-1-beta-D-ribofuranosylbenzimidazole (DRB) triggers p53-dependent apoptosis in human colon carcinoma cells. *Oncogene,* 18**,** 5765-72.

UHLMANN, T., BOEING, S., LEHMBACHER, M. & MEISTERERNST, M. (2007) The VP16 activation domain establishes an active mediator lacking CDK8 in vivo. *J Biol Chem,* 282**,** 2163-73.

WADA, T., TAKAGI, T., YAMAGUCHI, Y., FERDOUS, A., IMAI, T., HIROSE, S. *et al.* (1998) DSIF, a novel transcription elongation factor that regulates RNA polymerase II processivity, is composed of human Spt4 and Spt5 homologs. *Genes Dev,* 12**,** 343-56.

WANG, S. & FISCHER, P. M. (2008) Cyclin-dependent kinase 9: a key transcriptional regulator and potential drug target in oncology, virology and cardiology. *Trends Pharmacol Sci,* 29**,** 302-13.

WANG, W., YAO, X., HUANG, Y., HU, X., LIU, R., HOU, D. *et al.* (2013) Mediator MED23 regulates basal transcription in vivo via an interaction with P-TEFb. *Transcription,* 4**,** 39-51.

WOHLBOLD, L., LAROCHELLE, S., LIAO, J. C., LIVSHITS, G., SINGER, J., SHOKAT, K. M. *et al.* (2006) The cyclin-dependent kinase (CDK) family member PNQALRE/CCRK supports cell proliferation but has no intrinsic CDK-activating kinase (CAK) activity. *Cell Cycle,* 5**,** 546-54.

YAMAGUCHI, Y., TAKAGI, T., WADA, T., YANO, K., FURUYA, A., SUGIMOTO, S. *et al.* (1999) NELF, a multisubunit complex containing RD, cooperates with DSIF to repress RNA polymerase II elongation. *Cell,* 97**,** 41-51.

YANG, E., VAN NIMWEGEN, E., ZAVOLAN, M., RAJEWSKY, N., SCHROEDER, M., MAGNASCO, M. *et al.* (2003) Decay rates of human mRNAs: correlation with functional characteristics and sequence attributes. *Genome Res,* 13**,** 1863-72.

YANG, Z., ZHU, Q., LUO, K. & ZHOU, Q. (2001) The 7SK small nuclear RNA inhibits the CDK9/cyclin T1 kinase to control transcription. *Nature,* 414**,** 317-22.

ZHOU, Q., LI, T. & PRICE, D. H. (2012) RNA polymerase II elongation control. *Annu Rev Biochem,* 81**,** 119-43.

ZHU, Y., PE'ERY, T., PENG, J., RAMANATHAN, Y., MARSHALL, N., MARSHALL, T. *et al.* (1997) Transcription elongation factor P-TEFb is required for HIV-1 tat transactivation in vitro. *Genes Dev,* 11**,** 2622-32.

Table 1

Enzymatic kinase assay

	IC_{50} [µM]					
	CDK1-Cyclin B1	**CDK2-Cyclin A**	**CDK4-Cyclin D1**	**CDK6-Cyclin D3**	**CDK7-Cyclin H-MAT1**	**CDK9-Cyclin T1**
LDC000067	**5.513** ± 0.328 (n = 6)	**2.441** ± 0.227 (n = 6)	**9.242** ± 0.174 (n = 6)	**> 10** (n = 6)	**> 10** (n = 6)	**0.044** ± 0.010 (n = 6)
DRB	**> 10** (n = 1)	**> 10** (n = 1)	**> 10** (n = 1)	**> 10** (n = 1)	**> 10** (n = 1)	**1.942** (n = 1)
Flavopiridol	**< 0.005** (n = 3)	**0.015** ± 0.004 (n = 3)	**0.038** ± 0.008 (n = 3)	**0.305** ± 0.023 (n = 3)	**0.103** ± 0.023 (n = 3)	**0.0052** ± 0.0006 (n = 2)
SNS-032	**0.052** ± 0.009 (n = 3)	**0.006** ± 0.001 (n = 3)	**0.355** ± 0.017 (n = 3)	**3.404** ± 0.139 (n = 3)	**0.068** ± 0.008 (n = 3)	**0.0014** ± 0.0005 (n = 3)

Half-maximal inhibition (IC_{50}) of CDK inhibitors for the indicated CDK-cyclin pairs as determined by an *in vitro* enzymatic kinase assay using time-resolved FRET analysis.

Table 2

Kinase binding assay

	K_d [µM]		
	CDK2- **Cyclin A**	**CDK7-** **Cyclin H-MAT1**	**CDK9-** **Cyclin T1**
LDC000067	**1.014** ± 0.743 (n = 5)	**15.99** ± 8.919 (n = 5)	**0.0327** ± 0.0151 (n = 35)
DRB	n.d.	**> 10** (n = 2)	**0.614** ± 0.0269 (n = 2)
Flavopiridol	**0.0302** ± 0.0047 (n = 3)	**0.0963** ± 0.0114 (n = 8)	**< 0.005** (n = 8)

Dissociation constants (K_d) of CDK inhibitors 067, DRB and flavopiridol for the indicated CDKs were determined by an *in vitro* kinase activity assay. All reactions contained ATP at the concentration of the K_M of the individual kinases (CDK2-Cyclin A: 3 µM; CDK7-Cyclin H-MAT1: 25 µM; CDK9-Cyclin T1: 25 µM). N.d. = not determined.

Table 3

	Compound IC_{50} [nM]	
	LDC000067	**Staurosporine**
GSK3A	1460	4.21
HGK/MAP4K4	820	<1.0
ABL2/ARG	3640	6.42
CAMK4	>20000	28.90

Compounds were tested in 10-dose mode with 2-fold serial dilutions starting at 1000 µM for 067 and 3-fold serial dilutions starting at 20 µM for Staurosporine. Reactions were carried out at 1 µM ATP in a kinase catalytic activity assay containing kinase-specific substrates and cofactors (Anastassiadis *et al.*, 2011).

Figure legends

Figure 1

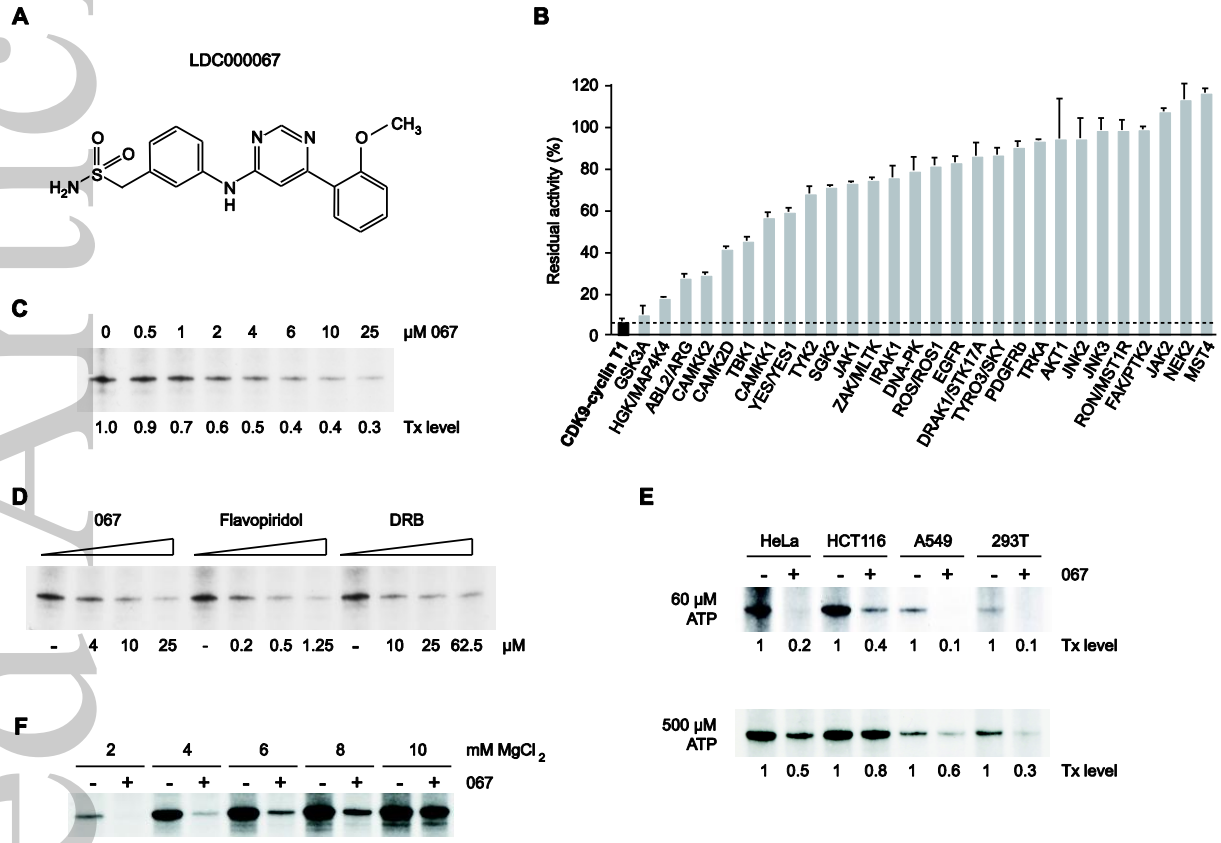

Figure 1

Inhibition of *in vitro* transcription by 067. **A.** Molecular structure of LDC000067. **B.** Inhibition of kinase catalytic activity by 10 µM 067. A radiometric *in vitro* kinase assay was used to determine residual kinase activity (expressed as percentage of remaining substrate phosphorylation compared to the DMSO control reaction). Each kinase was measured in duplicate, and bars/error bars indicate the mean/range of the two measurements. The stippled line indicates residual P-TEFb activity (6.2%) in this assay. **C.** and **D.** Influence of inhibitors on *in vitro* transcription using HEK293T nuclear extract. Transcripts originate from a 380 bp G-free cassette in pGal-ML. Transcript (Tx) levels were determined by phosphorimaging. **E.** Comparison of 067 effects in different nuclear extracts of the indicated cell lines under low (60 µM) and high (500 µM) ATP concentrations. Final inhibitor concentration was 10 µM. **F.**

Influence of magnesium on transcription inhibition by 067 (10 μM) with low ATP (60 μM) in HEK293T nuclear extract.

Figure 2

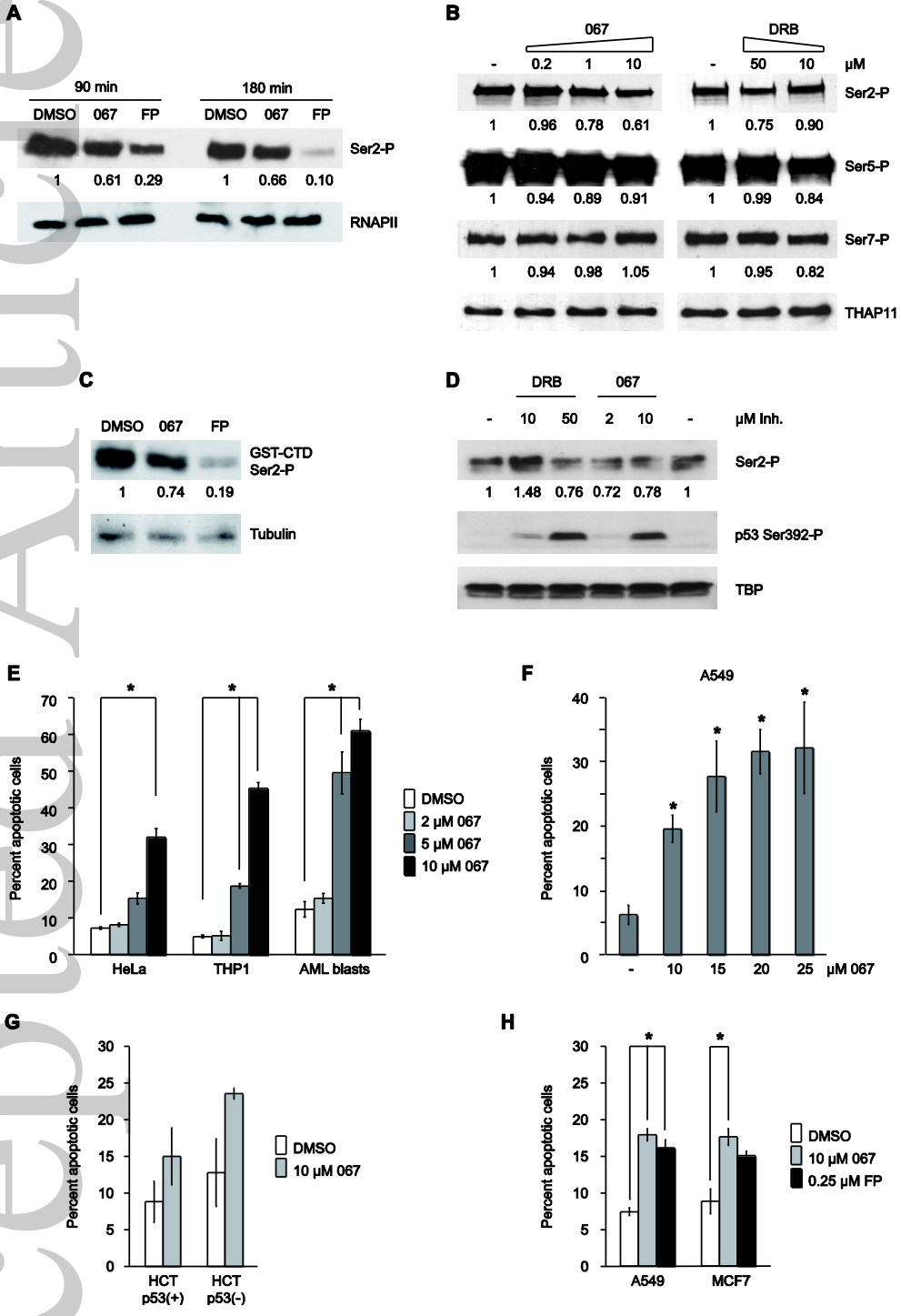

Figure 2

Cellular effects of CDK9 inhibition by 067. **A.** Western blot analysis of global Ser2-P levels in mESCs treated for 90 or 180 minutes with DMSO, 10 µM 067 or 1 µM flavopiridol (FP). Ser2-P signals were quantified using ImageJ (http://rsbweb.nih.gov/ij/) and normalized to RNAPII signals. B. Effects of CDK9 inhibitor treatment (60 min) in HeLa cells. THAP1

served as loading control. Quantification of CTD modifications was done as in A. C. Kinase assay using GST-CTD as substrate in HeLa nuclear extract treated with 10 µM 067 or 1 µM flavopiridol for 30 minutes. GST-CTD Ser2-P levels were quantified using ImageJ and Tubulin signals for normalization. D. MCF7 cells were treated for 4 hours with the indicated concentrations of CDK9 inhibitors and analysed by Western blot with the indicated antibodies. TBP served as loading control. **E** to **F.** Apoptosis induction in the indicated cell lines and patient-derived leukaemia (AML) blasts after 24 hours treatment. Apoptosis was assayed using flow cytometry of annexin V-propidium iodide double-stained cells. Signals are represented by the means ± standard deviations (error bars) of three biological replicates, except for AML blasts from a single patient, where three independent technical replicates were analysed. Student's t-tests were performed, and statistical significance was inferred when $p < 0.05$ (denoted as *).

Figure 3

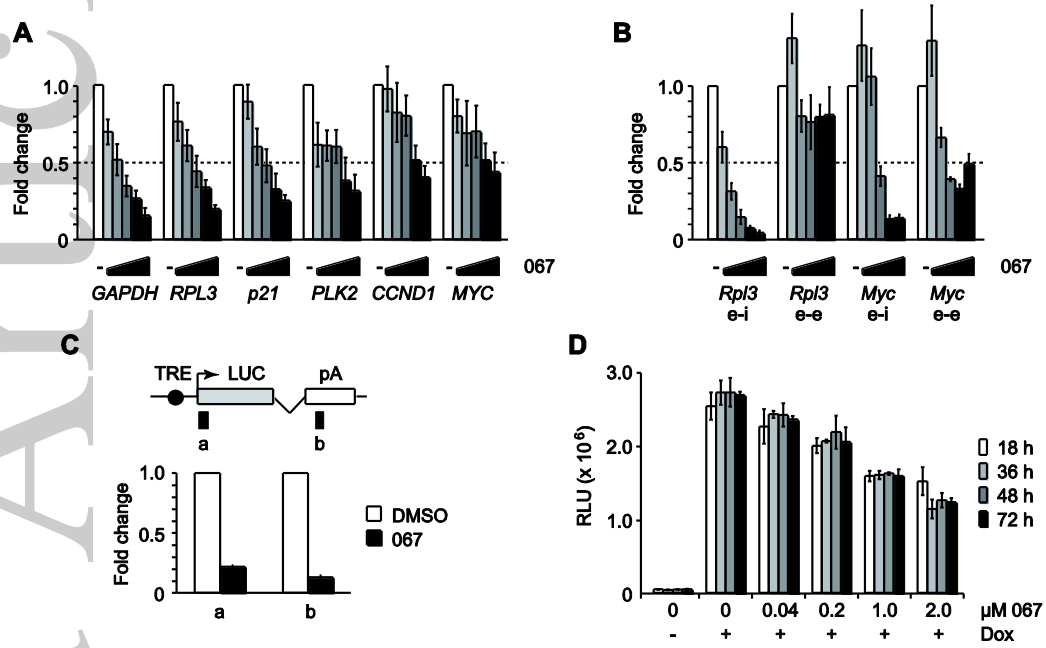

Figure 3

RT-qPCR analysis of *de novo* transcription. **A** and **B.** Increasing 067 concentrations (1/2/4/6/10 µM in A; 2.5/5/10/20/40 µM in B) were applied for 90 minutes and the indicated genes were analyzed in A549 cells (A) or mESCs (B) using exon-intron primers (e-i) and, for the latter, also exon-exon (e-e) primers. Half-maximal inhibition is indicated by the dotted line. **C.** RT-qPCR analysis of luciferase reporter gene transcripts in stably transfected HeLa cells treated with 10 µM 067 or DMSO for 30 minutes followed by 1 µg/ml doxycycline (Dox) for 60 minutes. Scheme of the luciferase (LUC) reporter gene and primer locations are shown at the top. **D.** Luciferase assay of Dox-induced HeLa reporter cells treated with increasing amounts of 067 for the indicated times.

Figure 4

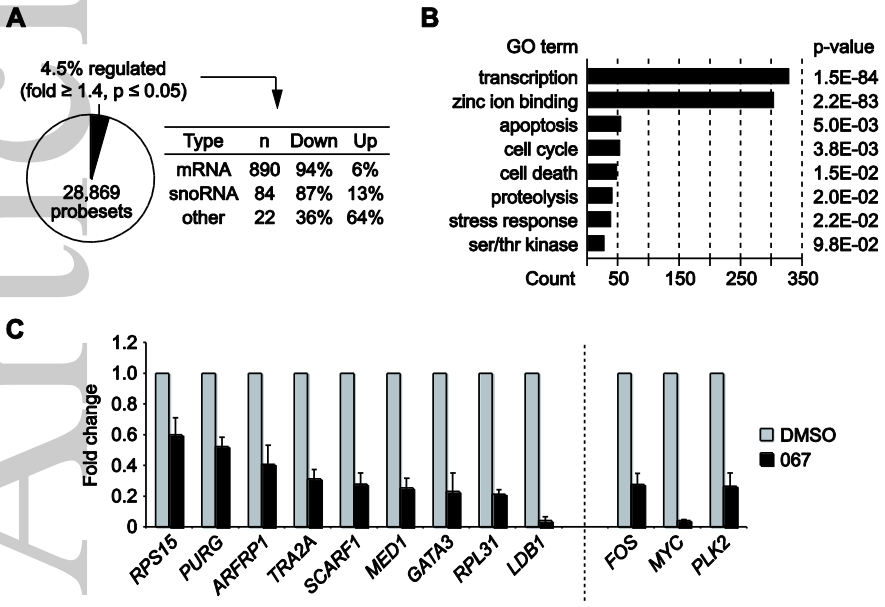

Figure 4

Microarray analysis of 067-treated THP1 cells **A.** Statistics of regulated genes. **B.** Gene ontology (GO) analysis of downregulated mRNAs. **C.** RT-qPCR analysis of unspliced *de novo* transcripts covering exon-intron sequences of the indicated genes in control or 067-treated THP1 cells. Genes to the left showed unchanged steady-state mRNA levels, while genes to the right (*FOS, MYC, PLK2*) were significantly downregulated in the microarray analysis.

Figure 5

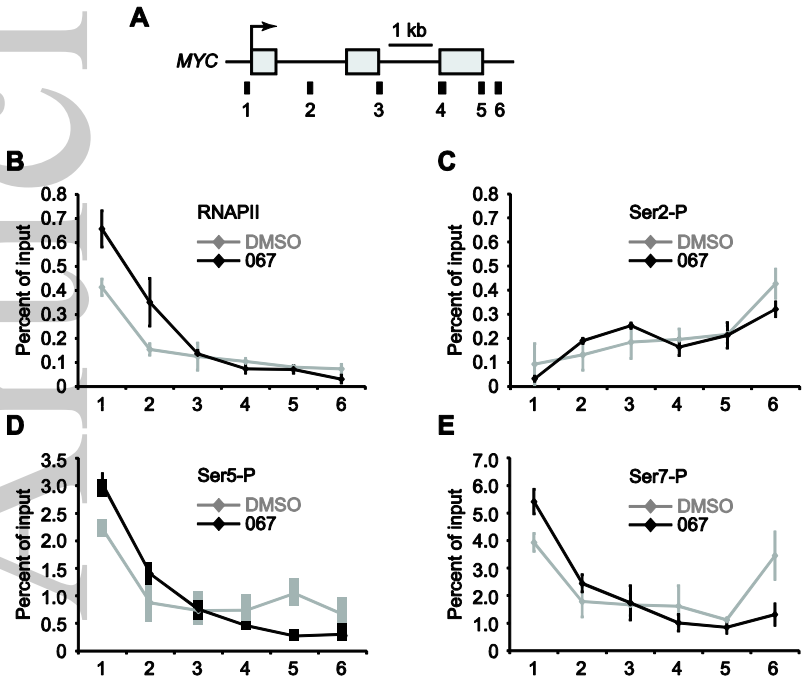

Figure 5

Increase of RNAPII pausing at *MYC* in the presence of 067. **A.** Scheme of the human *MYC* gene with qPCR amplicons used for ChIP analysis indicated underneath. Distribution of RNAPII (B), Ser2-P (C), Ser5-P (D) and Ser7-P (E) was determined by ChIP of HeLa cells treated with 10 µM 067 or DMSO for 1 hour.

Conflicts of interest

None.